Available online at www.sciencedirect.com

Carbohydrate Polymers 62 (2005) 113–119

Carbohydrate Polymers

www.elsevier.com/locate/carbpol

Preparation of novel chitosan scaffolds by electrochemical process

Yawo-Kuo Twu*, I-Tzu Chang, Chieh-Chung Ping

Department of Bioindustry Technology, Da-Yeh University, 112 Shan-Jiau Road, Da-Tsuen, Chang-Hua, Taiwan 51505, ROC

Received 12 November 2004; revised 22 June 2005; accepted 5 July 2005

Abstract

An electrochemical method of preparing chitosan scaffolds with three different molecular weights in various acid solutions has been reported. Chitosan samples prepared by electrolysis in acid solutions exhibited a rod-like geometry and a porous morphology with detectable deacetylation and degradation. The recovery rate of high molecular weight chitosan was highest among three polymers in all type of solvents. Specific gravity, crystallinity, and the morphology of various scaffolds were investigated by pycnometer, X-ray, and scanning electron microscopy studies. These evidences indicated that chitosan scaffolds lost some degree of crystallinity and showed a porous structure. The process and structures described here provided a starting point for the fabrication and design of chitosan based scaffold materials.

Keywords: Chitosan; Electrolysis; Scaffold; Porous structure

1. Introduction

Chitin is a natural polysaccharide found in a wide range of natural sources such as crustaceans, fungi, and insects. Chitosan is the N-deacetylated derivative of chitin (Shepherd, Reader, & Falshaw, 1997). Chitin and chitosan are chemically stable and widely used in agriculture, medicine, food, sewage treatment and functional fiber manufacture, etc. (Ravi Kumar, 2000). Chitosan has several polar groups such as –OH and $-NH_2$ which can act as electron donors. Chitosan is soluble as the salt in various acids. Chitosan with higher content of amino groups have been sought for the purpose of increasing their cationic content. Most polymers are excellent electrical insulators, and display high electrical resistance and very little conduction of an electric current. However, chitosan amine salts are capable of contributing electrical conductance either in an aqueous solution or in a solid state. Therefore, there are increased interests in studying the electrical properties of chitosan for a rapidly growing list of electrical and biological applications. Among these, most are concerned with the conductivity and electric resistance of chitosan. For example, the specific resistance (ρ) values of chitosan tablet decreased with increasing the water content and temperature. Chitosan tablets showed $\log\rho$values (8.7–9.0) at 20 °C and relative humidity (RH) = 50% (Suzuki, Saimoto, & Shigemasa, 1999). The conductivity of cast chitosan–salt complex films was due to the mobile ions from the salt and can be enhanced by plasticization (Osman, Ibrahim, & Arof, 2001). Relation between the degree of acetylation and the electrostatic properties of chitin and chitosan were also studied (Sorlier, Denuzière, Viton, & Domare, 2001). They concluded that chitosan and chitosan salts might be regarded as polycations which showed ionic conductivity.

Researchers also examined the mechano-electro-chemical (MEC) phenomenon and related performance of the chitosan/polymer fiber (Sun, Wong, Yao, & Mak, 2000). They found the fixed charge density on the chitosan chains may play an active role in the MEC process. Researchers also found that chitosan suspension showed the electrorheological response (Bingham fluid behavior) upon application of the electric field due to the polarizability of the branched amino polar group of the chitosan particles (Choi, 1999). Strong stochastic oscillations of electrical conductivity in swelled chitosan also have been reported (Ageev, Golub, & Vikhoreva, 1999). Application researches found that chitosan complex showed an electric stimulus-dependent stepwise bending behavior. Therefore, it could be useful for artificial organ components (Kim, Yoon, Lee, Park, & Kim, 2003). Good electrocatalytic properties of protein–chitosan

---

* Corresponding author. Tel.: +886 4 8511318; fax: +886 4 8511319.
E-mail address: poly2001@mail.dyu.edu.tw (Y.-K. Twu).

0144-8617/$ - see front matter © 2005 Elsevier Ltd. All rights reserved.
doi:10.1016/j.carbpol.2005.07.006

films have a promising potential in fabricating biosensors (Huang, Hu, Zeng, & Zhou, 2002). More works has also shown that the chitosan biopolymer can be a potential material in electrochromic devices (Yahya & Arof, 2004) and solid-state batteries (Morni & Arof, 1999; Subban, Arof, & Radhakrishna, 1996). There were so many studies that have reported the electrical properties and related applications of chitosan, however, there have been few studies about preparation of chitosan using electrochemical methods. The aim of this study was to develop a novel method for preparation of chitosan by electrolysis. The characterization of chitosan products was also reported.

2. Materials and methods

2.1. Materials

Chitosan, derived from crab shell, was a commercial powder supplied by QBAS Co. (Taiwan). Its viscosity average molecular weight *Mv* (Tsaih & Chen, 1997) was found to be 1540 kD. Its degree of deacetylation was determined to be 80% by the conductometric method for colloidal titration (Toei & Kohara, 1976). All other chemicals used for the following investigation were analytical grade and used without further purification. All aqueous solutions used in the experiments were made from deionized water.

2.2. Ultrasonic degradation of chitosan

Since chitosan is not soluble in water, we used acetic acid as the solvent for chitosan dissolution before it can be ultrasonicated. One-percent (w/v) chitosan in 5% (v/v) acetic acid aqueous solution were prepared. Three 500-mL of the solution in flasks were placed in a water bath at 60 °C and had a pH of 3.9. Ultrasonic treatments were conducted at 260 W for 5, 10, and 20 h with a sonicator (ULTRAsonic 57K, Degussa-Ney, USA), respectively. The samples were pippetted out and dropped into a 5% NaOH solution to be solidified and regenerated into particles. The solid materials were sufficiently washed in water until neutralized. The residues were collected and lyophilized. Three different molecular weight chitosans were obtained. Their viscosity average molecular weight *Mv* were found to be 1050 kDa (H-chitosan), 965 kDa (M-chitosan), and 615 kDa (L-chitosan), respectively.

2.3. Electrolysis of chitosan aqueous acid solutions

In a typical preparation of solution, 4 g chitosan was dissolved in 400 mL aqueous acid solution to form electrolyte solution. Attempts have been made to dissolve chitosan in phosphoric acid and hydrochloride acid. Both resulted in chitosan degradation and extensive hydrogen generation during electrolysis, therefore, these strong acids are not suitable as solvent for chitosan scaffolds preparation. Hence acetic acid ($ka = 1.75 \times 10^{-5}$) and formic acid ($ka = 1.8 \times 10^{-4}$) were used as solvents at different concentrations (0.05, 0.1, and 0.3 N) to dissolve H-, M-, and L-chitosan. The combinations of three chitosans and two acids with different concentrations resulted in 18 electrolyte solutions and 18 products (Table 1).

The electrolysis of chitosan solutions were performed in a $(L)100\ \text{mm} \times (W)80\ \text{mm} \times (H)80\ \text{mm}$ glass cell which has

Table 1
The charged composition of chitosan/acid electrolytes, product code, product average molecular weights and degree of deacetylation

Electrolyte solution	Chitosan[a]	Solvent[b]	Product code	Average molecular weight (kDa)	Degree of deacetylation (%)[c]
1	H-chitosan	0.05 N FA	HF-1	980	83
2	H-chitosan	0.1 N FA	HF-2	940	81
3	H-chitosan	0.3 N FA	HF-3	920	83
4	H-chitosan	0.05 N HAc	HA-1	1040	82
5	H-chitosan	0.1 N HAc	HA-2	1040	83
6	H-chitosan	0.3 N HAc	HA-3	1050	85
7	M-chitosan	0.05 N FA	MF-1	900	82
8	M-chitosan	0.1 N FA	MF-2	870	82
9	M-chitosan	0.3 N FA	MF-3	840	85
10	M-chitosan	0.05 N HAc	MA-1	940	82
11	M-chitosan	0.1 N HAc	MA-2	930	83
12	M-chitosan	0.3 N HAc	MA-3	930	85
13	L-chitosan	0.05 N FA	LF-1	540	84
14	L-chitosan	0.1 N FA	LF-2	540	83
15	L-chitosan	0.3 N FA	LF-3	500	83
16	L-chitosan	0.05 N HAc	LA-1	590	82
17	L-chitosan	0.1 N HAc	LA-2	580	84
18	L-chitosan	0.3 N HAc	LA-3	580	84

[a] 4 g chitosan in each 400 mL electrolyte solutions.
[b] Formic acid (FA) and acetic acid (HAc).
[c] From colloidal titration method.

two platinum electrodes (1 mm dia. × 90 mm length) and a power supplier TH-009 (MRL, Taiwan) having a constant voltage of 20 V at room temperature. Prior to each electrolysis the Pt electrodes surface were mechanically polished with a polishing cloth and rinsed with pure water in an ultrasonic cleaner. The process of electrolysis involved forcing a current through the cell to produce a chemical change that would not otherwise occur. The electrolysis of chitosan solution produced hydrogen gas at the cathode and oxygen gas at the anode. In the mean time, the effect of the electrolysis was to reduce chitosan-NH_3^+ ions to neutral molecules that form solid chitosan on the cathode. It was observed that chitosan started depositing on the cathode immediately passing the electrical current. However, the electrical current decreased as the process continued. This is most likely the result of low conductivity of chitosan on the cathode which inhibited the electrolysis as well as the formation of chitosan scaffold. Prolonging the reaction time was not an effective method for increasing recovery of chitosan from the cell. For comparing the recovery rate of each reaction, the deposited chitosan scaffolds were removed from cathode and the reaction was continually repeated every hour. This process was repeated 10 times and most of chitosan was recovered from the cell. The recovered chitosan was rinsed with distilled water and dried in a freeze dryer.

2.4. Characterization

The digital photographs of chitosan scaffolds were taken with a Kodak digital camera DC-3400 (Kodak, Japan). Their viscosity molecular weights were measured and calculated based on the Mark Houwink equation (Tsaih & Chen, 1997). The degrees of deacetylation were determined by the conductometric method for colloidal titration (Toei & Kohara, 1976). The specific gravity of scaffolds were measured in a pycnometer at 25 °C according to ASTM D 792 method B. XRD pattern were measured with a MAC Science X-ray diffractometer MXP-18 (MAC Science, Japan) with Ni-filtered Cu Kα radiation at 12 kV and 50 mA. The surface and cross-sectional morphologies were examined from micrographs taken with a scanning electron microscopy (SEM, TOPCON ABT150S, Japan). Samples were mounted on metal grids and coated with gold under vacuum before observation.

3. Results and discussion

3.1. Chitosan scaffolds preparation

Chitosan degradation increased with prolonged ultrasonic time, while the degree of deacetylation was maintained. In preliminary studies, molecular weight of 1540 and 100 kD chitosans solutions were electrolyzed. It seemed surprising that for these solutions to chitosan scaffolds were not obtained. A possible explanation is the slow motion of high molecular weight chitosan in cell and redissolution of deposited chitosan in acidic solution that caused extremely low yields. On the other hand, the low molecular weight chitosan were highly soluble in acid and thus the deposited chitosan were redissolved before it could be obtained. These experiments revealed the limitation of chitosan molecular weight in forming scaffolds by electrolysis and will be further studied.

In this study, molecular weight of 1050 kDa (H-chitosan), 965 kDa (M-chitosan), and 615 kDa (L-chitosan) of similar degree of deacetylation were used. It is very important to note that hydrogen and oxygen were produced during electrolysis. The electric current actually not only caused the deposition of chitosan at the cathode but also caused the water molecules to dissociate, thus producing hydrogen gas at the cathode and oxygen gas at the anode. Hydrogen bubble adhered on chitosan until it rose from the scaffolds. This put voids inside the scaffold. As can be seen from Fig. 1, the dried scaffolds were porous and about 6 cm in length without shrinkage. The pore sizes were within the range of 0.5–2 mm. This was most likely the result of the voids and not the result of the freeze-drying which usually has a pore size within the range of 1–250 μm (Madihally & Matthew, 1999).

3.2. Effect of the type of solvent

Fig. 1A–C show the H-chitosan scaffolds prepared from 0.05, 0.1 and 0.3 N acetic acid solutions, respectively. As it may be seen, HA-1 chitosan scaffold prepared from 0.05 N acetic acid solution was about 14.5–20 mm in diameter and 1.63 g in weight, which was large compared to HA-2 (10–14 mm dia., 0.82 g) and HA-3 (4–11 mm dia., 0.32 g). The length of all products was about 6 cm. As it may be seen, the recovery of H-chitosan decreased dramatically as the concentration of acid increased. During electrolysis, water was decomposed into hydrogen and oxygen gas. It could be collected by water displacement. There was fewer than 10 mL hydrogen gas which was collected during preparation of HA-1. While on the contrary, there were more than 60 ml and 100 mL hydrogen gas which were collected during preparation of HA-2 and -3, respectively. This would suggest that the dissociation of water was predominant in higher acid concentration solution. Since the amount of water decomposed was less than 1 mL in all the cases, the variation of acid concentration was negligible.

In order to study the recovery rate of chitosan, we removed chitosan scaffold from the cathode and repeated the same electrolysis procedure every hour. This process was repeated 10 times until most of chitosan was recovered from cell. Chitosan should be removed from cathode after a time because of lower conductivity chitosan scaffold on the surface of cathode that decreased the electrolysis rate. The recovery rate was calculated

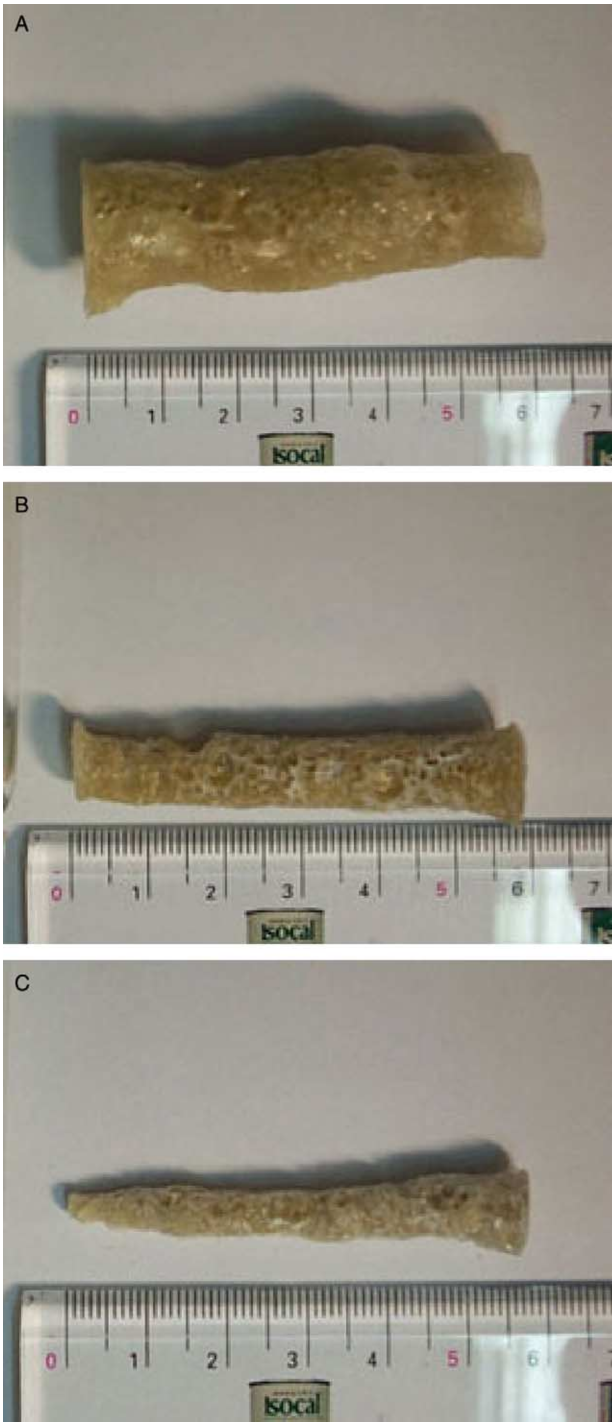

Fig. 1. Digital photographs of chitosan scaffolds: (A) HA-1; (B) HA-2 and (C) HA-3.

using the following equation:

$$\text{Recovery rate}(\%) = [\text{accumulated scaffold weight}(g)/4(g)]100\%$$

After 10 repetitions, the accumulated scaffold weights were within the range of 3.19–2.04 g. This mean that there were 20–50% chitosan was still in the cell. Fig. 2A and B show the accumulated recovery rate of chitosan from acetic acid and formic acid solutions, respectively. As it may be seen, the recovery rate decreased as acid concentration increased as well as the chitosan molecular weight decreased in both acetic acid and formic acid solutions. At the beginning of electrolysis, the relative higher amount of chitosan was recovered from a 0.04 N acid solution then the amount retrieved was decreased dramatically every other hour. In the meantime, the recovery rate of chitosan was decreased gradually from the 0.1 N acid solution and was about same from the 0.3 N acid solution. Eventually, the difference of accumulated recovery rates among various concentrations was not as significant as we would expect from Fig. 1. Nonetheless, we found that the recovery rate of H-chitosan was highest among three polymers. This reaffirmed that H-chitosan had better deposition on the cathode and lower solubility in acid solution.

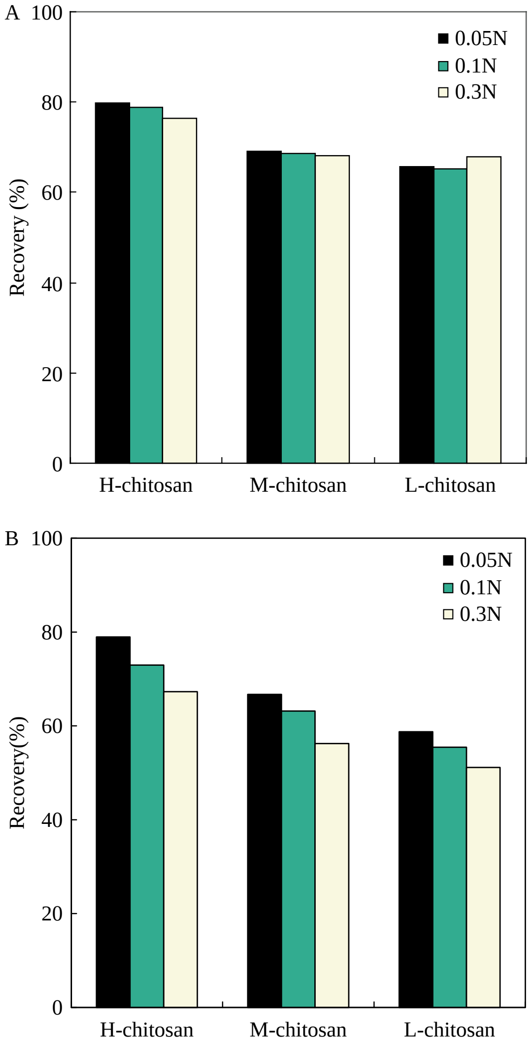

Fig. 2. The recovery rate of chitosan from (A) acetic acid solution and (B) formic acid solution.

Comparing Fig. 2A with B, we found chitosan recovery rates were higher in acetic acid solutions than formic acid solutions. We had collected more hydrogen gas from formic acid solution than from acetic acid solution during electrolysis. For examples, we collected about 10, 60, and 100 mL H_2 during preparation of HA-1, -2, and -3, respectively. In the mean time, we collected 22, 89, and 127 mL H_2 during preparation of HF-1, -2, and -3, respectively. We checked the acid dissociation constants at 25 °C. It is not surprising, that the dissociation constant of formic acid (1.80×10^{-4}) is higher than that of acetic acid (1.75×10^{-5}) at room temperature. Since the H^+ was reduced in both acid solution, the higher H^+ concentration the more hydrogen gas generated. This was why we observed more H_2 generated from formic acid solutions. There was a competition between H_2 generation and chitosan deposition. In the mean time, the generation of H_2 bubble also disturbed the formation of chitosan scaffold. The high H^+ concentration solutions will not be used in future studies.

3.3. Characterization of chitosan scaffolds

Table 1 shows the effect of electrolysis on changes of molecular weight and degree of deacetylation. The molecular weights of chitosan scaffolds prepared from acetic acid solutions decreased slightly. However, the molecular weight of chitosan scaffolds prepared from formic acid solution decreased by 5–10%. The formic acid characteristics have a considerable effect on the hydrolysis of chitosan during electrolysis. The electrolysis led to detectable deacetylation (1–5%), which may be because, the electrolysis provides the added energy needed to break the molecular main chain as well as side bonds.

Apparent densities of chitosan scaffolds including voids inherent in the material were in the range of 0.12–0.14 g/cm^3. However, the density of solid chitosan scaffold flake measured in a pycnometer at 25 °C according to ASTM D 792 method B (Shan, 1984) was 1.1 g/cm^3. When voids were included, the total porosities of chitosan scaffolds were about 90% by calculation. X-ray analyses of chitin powder, the original chitosan powder, and the scaffolds were performed in order to characterize the physical state of the polysaccharides. The crystallinity of the chitosan scaffolds was lower than the crystallinity of the chitin powder and original chitosan powder (Fig. 3). These results suggested that the electrolysis may be too fast a phase inversion process for the chitosan to allow crystallization. The diffraction of chitosan scaffolds also decreased as the concentration of acid solution increased. The interaction between concentrated H^+ and the chitosan molecule reduced crystalline structure and a lower crystallinity scaffold was obtained. The specific gravity and X-ray diffraction measurement suggested that affluent chitosan molecule deposition was obtained by using the electrolysis process.

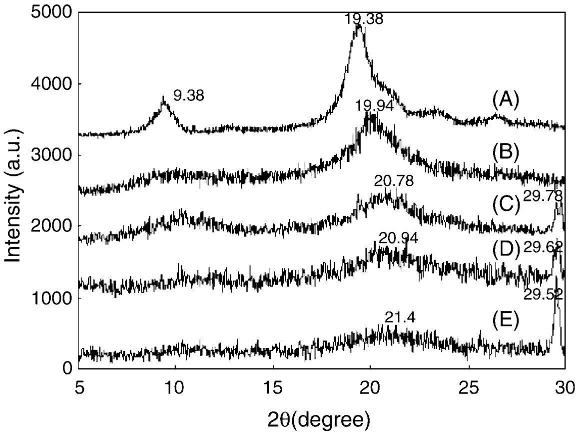

Fig. 3. X-ray diffraction diagrams of chitin and chitosan: (A) chitin powder; (B) chitosan powder; (C) HA-1; (D) HA-2 and (E) HA-3.

As it may be seen on Fig. 1A–C, chitosan scaffolds including voids inherent were showing. Fig. 4A and B show high-magnification (×2000) solid chitosan flake surface morphology of HA-1 and HF-1, respectively. Both images

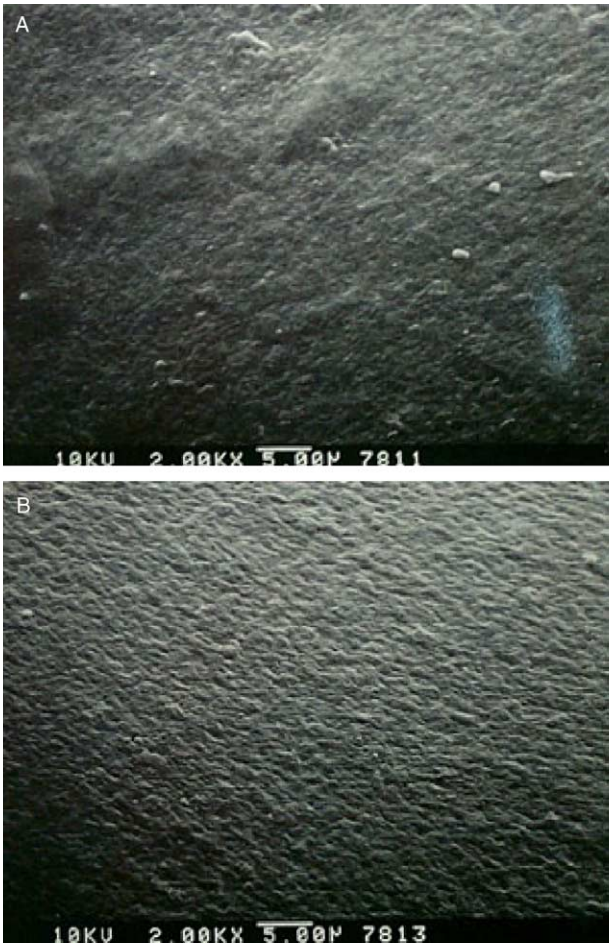

Fig. 4. SEM micrographs of chitosan scaffolds: (A) HA-1 (×2000) and (B) HF-1 (×2000).

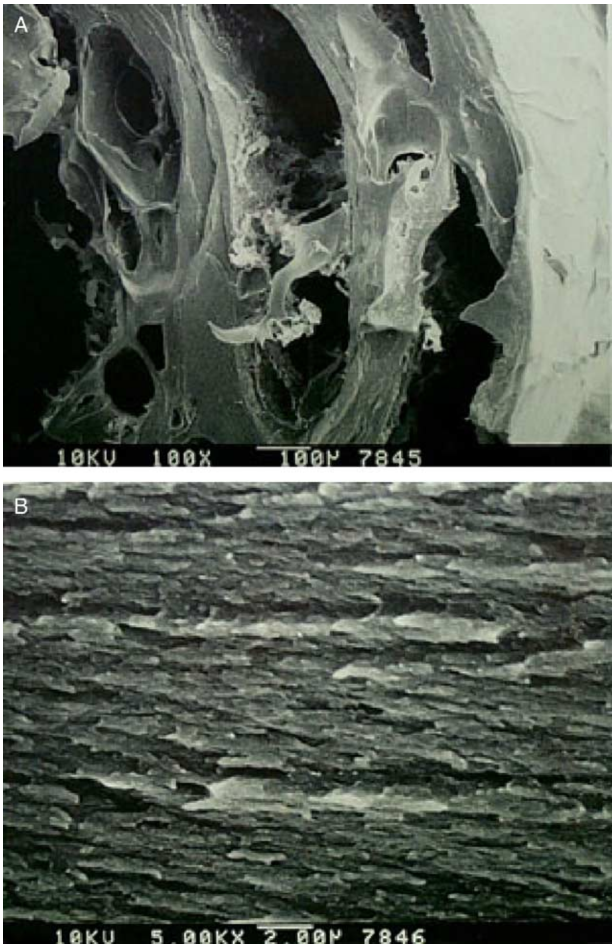

Fig. 5. SEM micrographs of cross-section of chitosan scaffolds: (A) HA-1 (×100)and (B) HA-1 (×5000).

exhibited that no opening or empty space were bigger than 1 μm. Fig. 5A shows a low-magnification (×100) sectional view of chitosan scaffolds. The electrolysis process generated hydrogen gas and left voids which joined onto one another in the bulk scaffold. From the density calculation, these open pore structures inhabited about 90% by volume of chitosan scaffolds. In contrast Fig. 5B, a high-magnification (×5000) sectional view of chitosan scaffold, shows a laminar and orientated morphology. Figs. 1, 4 and 5 summarized the typical effect of electrolysis on the repacking of chitosan molecules. Taken as a whole, chitosan molecules moved to the cathode in parallel while hydrogen was generated during electrolysis. Most of gas escaped from cathode, but part of gas was trapped inside chitosan scaffold. In comparison to solution casting method, deposition of chitosan in an electrolytic cell is a quick method and the diversified shape could approach the users' favor. Casting methods usually produce smooth surface. However, performance of varied biofunctions usually demands a porous structure. Our method may be useful for some bioapplications.

4. Conclusions

The solutions of chitosan in acetic acid and formic acid have been found suitable for the preparation of novel chitosan scaffolds by electrolysis. It should be noted that slightly different characteristics might be obtained depending on the variability of the chitosan solutions (type of acid, chitosan molecular weight, acid concentration, or else). We found the recovery rate of H-chitosan was highest among three polymers in all type of solvents. The effect of electrolysis on changes in chitosan molecular weight and degree of deacetylation were detectable. The X-ray evidence indicates that the final products were actually losing some crystallinity because of low phase inversion rate for the chitosan molecules to allow crystallization. These chitosan scaffolds were porous structure with pore sizes in the range of 0.5–2 mm. The methods and structures described here provide a novel point for use of chitosan in future applications.

Acknowledgements

This work was financially supported in part by a grant No. 90-2313-B212-004 from the National Science Council of Republic of China. The SEM and X-ray assistance from Regional Instruments Center at NCHU, are gratefully acknowledged.

References

Ageev, Y. P., Golub, M. A., & Vikhoreva, G. A. (1999). Stochastic autooscillations of electrical conductivity of chitosan films swelled in water. *Materials Science and Engineering C*, *8–9*, 373–376.

Choi, U.-S. (1999). Electrorheological properties of chitosan suspension. *Colloids and Surfaces A*, *157*, 193–202.

Huang, H., Hu, N., Zeng, Y., & Zhou, G. (2002). Electrochemistry and electrocatalysis with heme proteins in chitosan biopolymer films. *Analytical Biochemistry*, *308*, 141–151.

Kim, S. J., Yoon, S. G., Lee, K. B., Park, Y. D., & Kim, S. I. (2003). Electrical sensitivity behavior of a polyelectrolyte complex composed of chitosan/hyaluronic acid. *Solid State Ionics*, *164*, 199–204.

Madihally, S. V., & Matthew, H. W. T. (1999). Porous chitosan scaffolds for tissue engineering. *Biomaterials*, *20*, 1133–1142.

Morni, N. M., & Arof, A. K. (1999). Chitosan–lithium triflate electrolyte in secondary lithium cells. *Journal of Power Sources*, *77*, 42–48.

Osman, Z., Ibrahim, Z. A., & Arof, A. K. (2001). Conductivity enhancement due to ion dissociation in plasticized chitosan based polymer electrolytes. *Carbohydrate Polymers*, *44*, 167–173.

Ravi Kumar, M. N. V. (2000). A review of chtin and chitosan applications. *Reactive and Functional Polymers*, *46*, 1–27.

Shan, V. (1984). *Handbook of plastics testing technology*. New York: Wiley.

Shepherd, R., Reader, S., & Falshaw, A. (1997). Chitosan functional properties. *Glycoconjugate Journal*, *14*, 535–542.

Sorlier, P., Denuzière, A., Viton, C., & Domare, A. (2001). Relation between the degree of acetylation and the electrostatic properties of chtin and chitosan. *Biomarcromolecules*, *2*, 765–772.

Subban, R. H. Y., Arof, A. K., & Radhakrishna, S. (1996). Polymer batteries with chitosan electrolyte mixed with sodium perchlorate. *Materials Science and Engineering*, *B38*, 156–160.

Sun, S., Wong, Y. W., Yao, K., & Mak, A. F. T. (2000). A study on mechano-electro-chemical behavior of chitosan/poly(propylene glycol) composite fibers. *Journal of Applied Polymer Science*, *76*, 542–551.

Suzuki, K., Saimoto, H., & Shigemasa, Y. (1999). Electric resistance of chitosan derivatives. *Carbohydrate Polymers*, *39*, 145–150.

Toei, K., & Kohara, T. (1976). A conductometric method for colloid titrations. *Analytica Chimica Acta*, *83*, 59–65.

Tsai, M. L., & Chen, R. H. (1997). Effect of molecular weight and urea on the conformation of chitosan molecules in dilute solution. *International Journal of Biological Macromolecules*, *20*, 233–240.

Yahya, M. Z. A., & Arof, A. K. (2004). Conductivity and X-ray photoelectron studies on lithium acetate doped chitosan film. *Carbohydrate Polymers*, *55*, 95–100.